Journal of Hydrology 519 (2014) 1084–1096

Contents lists available at ScienceDirect

Journal of Hydrology

journal homepage: www.elsevier.com/locate/jhydrol

Modelling vegetation water-use and groundwater recharge as affected by climate variability in an arid-zone *Acacia* savanna woodland

Chao Chen [a,b,c,*], Derek Eamus [a,b,d,e], James Cleverly [b,e], Nicolas Boulain [b], Peter Cook [a,f], Lu Zhang [g], Lei Cheng [g], Qiang Yu [b]

[a] National Centre for Groundwater Research and Training (NCGRT), School of Environment, Flinders University, Adelaide, SA 5001, Australia
[b] Plant Biology and Climate Change Cluster, University of Technology Sydney, PO Box 123, Broadway, NSW 2007, Australia
[c] CSIRO Agriculture Flagship, PMB 5, PO Wembley, WA 6913, Australia
[d] NCGRT, University of Technology Sydney, Australia
[e] Australian Supersite Network, Terrestrial Ecosystem Research Network, University of Technology Sydney, Australia
[f] Water for a Healthy Country National Flagship, Commonwealth Scientific and Industrial Research Organisation, Division of Land and Water, Glen Osmond, Adelaide, SA 5064, Australia
[g] CSIRO Land and Water Flagship, Canberra, ACT 2601, Australia

ARTICLE INFO

Article history:
Received 10 April 2014
Received in revised form 15 July 2014
Accepted 14 August 2014
Available online 21 August 2014
This manuscript was handled by Peter K. Kitanidis, Editor-in-Chief, with the assistance of Ty Ferre, Associate Editor

Keywords:
Climate variability
Groundwater recharge
Savanna woodland
Vegetation water-use
WAVES

SUMMARY

For efficient and sustainable utilisation of limited groundwater resources, improved understanding of how vegetation water-use responds to climate variation and the corresponding controls on recharge is essential. This study investigated these responses using a modelling approach. The biophysically based model WAVES was calibrated and validated with more than two years of field experimental data conducted in Mulga (*Acacia aneura*) in arid central Australia. The validated model was then applied to simulate vegetation growth (as changes in overstory and understory leaf area index; LAI), vegetation water-use and groundwater recharge using observed climate data for the period 1981–2012. Due to large inter-annual climatic variability, especially precipitation, simulated annual mean LAI ranged from 0.12 to 0.35 for the overstory and 0.07 to 0.21 for the understory. These variations in simulated LAI resulted in vegetation water-use varying greatly from year-to-year, from 64 to 601 mm pa. Simulated vegetation water-use also showed distinct seasonal patterns. Vegetation dynamics affected by climate variability exerted significant controls on simulated annual recharge, which was greatly reduced to 0–48 mm compared to that (58–672 mm) only affected by climate. Understanding how climate variability and land use/land cover change interactively impact on groundwater recharge significantly improves groundwater resources management in arid and semi-arid regions.

1. Introduction

Groundwater is a valuable natural resource, which not only supports human activities, but also has a key role in sustaining the health of wide-spread groundwater dependent ecosystems (Eamus et al., 2006; Jha et al., 2007). Sustainable water resource management is a major challenge for water resource managers in arid and semi-arid regions (Fernandez et al., 2002), where excessive and unsympathetic groundwater abstraction can degrade ecosystem function (Clifton and Evans, 2001; Donohue et al., 2007). Vegetation dynamics in arid and semi-arid regions largely depend on soil water availability, which in turn, result in a number of complex hydrologic processes (Gee et al., 1994; Porporato et al., 2002; Scanlon et al., 2005; Garcia et al., 2011). Climate variations, which lead to changes in vegetation structure and/or its water-use, can have a major impact on recharge to groundwater because transpiration is a major component of catchment water balances, to which biological productivity is intimately coupled (Berry et al., 2005; Chen et al., 2010). Understanding the effects of climate variations on vegetation water-use and groundwater recharge is particularly important in arid and semi-arid regions, where limited water resource availability is a major factor constraining regional development. Similarly, climate change is a growing concern for water management globally, including Australia because of the potential for declines in water supplies.

Studies of these complex problems can be conducted in field conditions and much has been learnt about the relationship among

* Corresponding author at: National Centre for Groundwater Research and Training (NCGRT), School of Environment, Flinders University, Adelaide, SA 5001, Australia. Tel.: +61 0295148405.
E-mail addresses: ccchenchao2009@163.com, chao.chen@csiro.au (C. Chen).

http://dx.doi.org/10.1016/j.jhydrol.2014.08.032
0022-1694/

growth, photosynthesis and the water cycle (Farrington, 1989; Thorburn et al., 1993; Zhang and Schilling, 2006). However, field experiments are time consuming, relatively expensive and difficulties in up-scaling from limited numbers of observations are apparent (Singh et al., 2006). To overcome this, process-based models that link hydrology and plant ecophysiology have been developed that provide useful tools to investigate interactions amongst energy, water and momentum balances of the soil–vegetation-atmosphere system across multiple spatial and temporal scales (Baird et al., 2005; Guswa et al., 2002; Laio et al., 2001). Studies of modelling these coupled behaviours have been attempted previously (Zhang et al., 1999a; Gerten et al., 2004; Kucharik et al., 2000). For example, Barron et al. (2012) modelled the effects of climate on recharge across Australia and found that the role of climate drivers varied across soil and vegetation types, while Crosbie et al. (2011) reported that recharge in the Murray–Darling Basin would be increased despite a modelled decrease in rainfall, due to the effect of increased temperature stress on vegetation growth. Although these studies provide useful information for developing applicable water management practices, there is still a lack of systematic analysis of the effects of climate variability on vegetation water-use and consequential recharge in arid and semi-arid regions.

Mulga (*Acacia aneura* and related species) is a low-to-medium height (2–8 m) tree, dominating arid and semi-arid zones between approximately 20 °S and 31 °S in coastal Western Australia and throughout the continental interior. Mulga occupies almost 20% of the Australian continent and overlies many significant aquifers including the Great Artesian Basin. Covering such a large portion of continental Australia, vegetation water-use and recharge beneath the Mulga-dominated woodland are assumed to contribute significantly to regional water budgets (Eamus et al., 2013). Mulga is functionally a savanna as it consists of a discontinuous tree layer over a grassy understory with highly seasonal rainfall. This pattern is more pronounced in arid central Australia where rainfall variability is skewed towards very large event cycles (Berry et al., 2011; Morton et al., 2011). Some studies have shown that, in this water-limited environment Mulga plays an important role in controlling water fluxes, including runoff, infiltration and groundwater recharge (Perry, 1970; Dunkerley, 2002; Berg and Dunkerley et al., 2004). However to-date, no studies have quantified the responses of groundwater recharge to Mulga-dominated vegetation under variable climate in arid and semi-arid regions. Such knowledge of the magnitude of recharge is critical to the development of sustainable strategies to allocate limited groundwater.

The objective of this study was to produce a detailed mechanistic understanding of the dynamic links between vegetation water-use and climate, and their influence on groundwater recharge through application of a physiologically-based model of the soil–plant–atmosphere continuum. The primary purpose of this study was to test the hypothesis that recharge of groundwater is largely dependent on the rate of water-use of vegetation growing in an arid region of Australia. The aims of this study were to: (1) parameterise the WAVES model to allow simulation of plant growth and water balance components in the Ti-Tree Basin using field data; (2) quantify the responses of plant growth and vegetation water-use to climate variability and the corresponding effects on groundwater recharge.

2. Materials and methods

2.1. Study site

This study was performed in the Ti-Tree Basin, located 150 km north of Alice Springs, in the Northern Terrority of Australia (Fig. 1). The basin is approximately 5500 km^2, and comprises undulating sand plains with alluvial deposits along ephemeral drainage lines. Vegetation includes large areas of spinifex under sparse woodland of Corymbia opaca and low trees, including *Acacia coriaceae* and *Hakea macrocarpa*. The sand plains contain patches of Mulga (*A. aneura*) and the major rivers are lined with River Red Gums (*Eucalyptus camaldulensis var. obtusa*). Over most of the basin, the water table is between 20 and 50 m below the land surface. Due to low rainfall, groundwater is an important resource for stock, irrigation of small-scale horticultural cropping, and town and community supplies. Therefore recharge to the groundwater needs to be determined to ensure that the resource is properly managed.

The study site is located on the western margin of the Ti-Tree Basin (22.28S, 133.25E, a.s.l. 600 m) (Fig. 1). The climate is characterised as having hot summers and warm winters. Average annual rainfall at the nearest meteorological station (Territory Grape Farm Station) is approximately 333 mm, much lower than annual pan evaporation of 3109 mm. The ecosystem is a savanna woodland with an average canopy height of 6.5 m, which consists of a discontinuous tree layer over a grassy understory. The soil is characterised as a red kandosol (sand:silt:clay 74:11:15).

2.2. Data for model testing

2.2.1. Climate data

An eddy covariance (EC) tower was located on a flat plain between the Hanson and Woodforde Rivers, being a member of the OzFlux network (Cleverly, 2011). Potential fetch is 11 km to the east and 16 km to the south. EC data collection was initiated on 2 September 2010. Total solar radiation was measured 12.2 m above the ground with a CNR1 (Kipp & Zonen, Delft, The Netherlands). Air temperature and relative humidity were measured 11.6 m above the ground using an HMP45C (Vaisala, Helsinki, Finland). Precipitation was measured with a CS7000 (Hydrologic services, Warwick, NSW, Australia), centred in a 10 m × 15 m clearing at the top of a 2.5 m mast. Frequency of micrometeorological measurements was 10 Hz with a 30-min covariance interval.

2.2.2. Soil data

Soil samples were collected using a slide hammer (AMS Soil Core Sampler, Envco: The Environmental Collective, Auckland, New Zealand) to extract intact cores (38 mm diameter × 10 cm depth to a maximum depth of 1.4 m) for laboratory analysis. The experimental site had a fairly uniform soil profile and dry bulk density varied only slightly, ranging from 1.67 g cm^{-3} at the surface to 1.86 g cm^{-3} at 1.4 m depth. Consequently we assumed that the soil could be simulated as a single layer. A soil column of 4 m was chosen considering a relatively shallow rooting depth for Mulga, which was shown not to access soil water below 5 m, even in drought conditions (Hill and Hill, 2003; Anderson et al., 2008). Soil hydraulic characteristics required by the model (Table 1) were derived from the ASRIS v1 database (Johnston et al., 2003). Soil moisture was measured in two vertical arrays under Mulga and understory habitats using TDR probes (CS610, Campbell Scientific, Townsville, Australia). Insertions with the 45° angle were at 10, 60 and 100 cm representing average soil moisture across depths of 10–30, 60–80 and 100–120 cm, respectively. For model calibration (see below), soil water was averaged without weighting across Mulga trees and understory grasses.

2.2.3. LAI data

Although knowledge of leaf area index (LAI) is vital to any mechanistic understanding of the hydrological role of vegetation (Eamus et al., 2006), it is difficult to measure across large spatial scales and difficult to simulate due to spatial and temporal variability. To assess model performance, the simulated total LAI

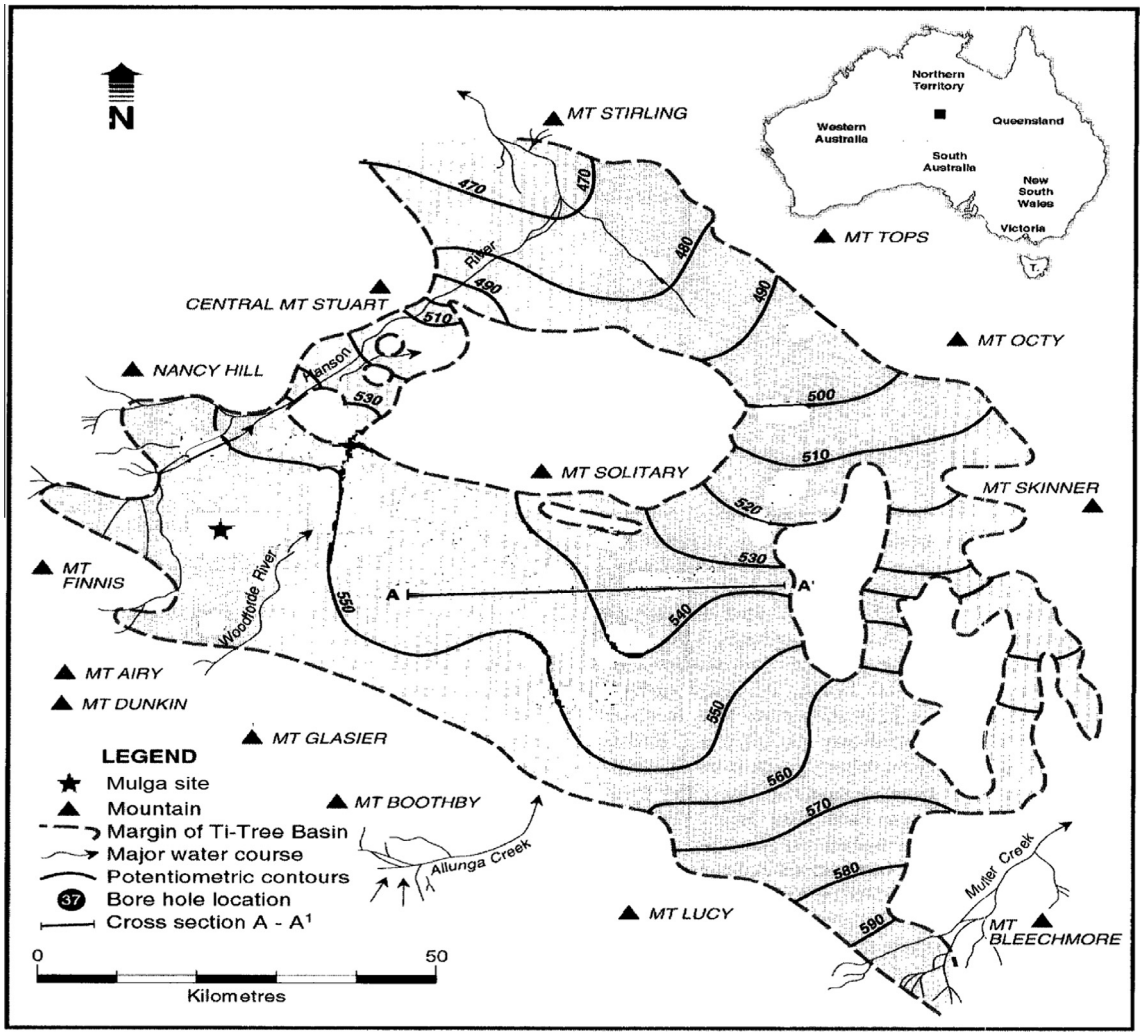

Fig. 1. The Ti-Tree Basin, central Australia (small black square on inset map) and the study site (Modified from Harrington et al., 2002). Potentiometric contours indicate the general direction of groundwater flow is to the east and north from the western and southern margins, respectively.

Table 1
Soil layer and parameters estimated for the soil model simulations.

Soil layer	Soil depth (m)	Texture	*Ks* (m d^{-1})	θ_s (cm^{-3} cm^{-3})	θ_d (cm^{-3} cm^{-3})	λc (m)	*C*
1	0–4	Sandy loam	1.0	0.33	0.06	0.04	1.02

Ks, saturated hydraulic conductivity.
θ_s, saturated soil water content.
θ_d, air-dry volumetric water content.
λc, characteristic length.
C, shape parameter related to soil texture and structure.

(over storey plus understory) was compared to field-measured LAI and MODIS LAI (Fig. 2). Field-measured LAI was derived from images acquired with a digital camera (Canon DSLR) equipped with a short focal lens (18 mm). Five 100 m long transects in E, SE, S, SW and W directions were established around the flux tower. Upward and downward images were taken every 10 m. To compute LAI, images were acquired with the camera looking to the sky at the nadir (0°) and at the soil at 57.5° from the vertical (Weiss et al., 2004) for overstory and understory, respectively. These images for overstory were analysed with a Matlab (Matlab R2012, The Mathworks, Natick, MA, USA) program based on algorithms obtained from MacFarlane et al. (2007), and those for understory were analysed with the CANEYE (version 6.3) software (https://www4.paca.inra.fr/can-eye). Overstory LAI was calculated from the fraction of foliage and crown covers for each image, while understory LAI was computed and corrected using the clumping index derived from fisheye images (MacFarlane et al., 2007). Total LAI calculated as the sum of the overstory and understory components was compared to the product MOD15A2 centred on the coordinate of the tower (8-Day Composite (Collection 5), 1 km wide × 1 km length) from the MODIS Land Product Subsets project (http://daac.ornl.gov/MODIS/). To ensure the highest quality, the 8-day composite LAI product was used only when QC filter conditions (FparLai QC < 32) were met.

A more detailed description of the study site and measurements can be found in Cleverly et al. (2013) and Eamus et al. (2013).

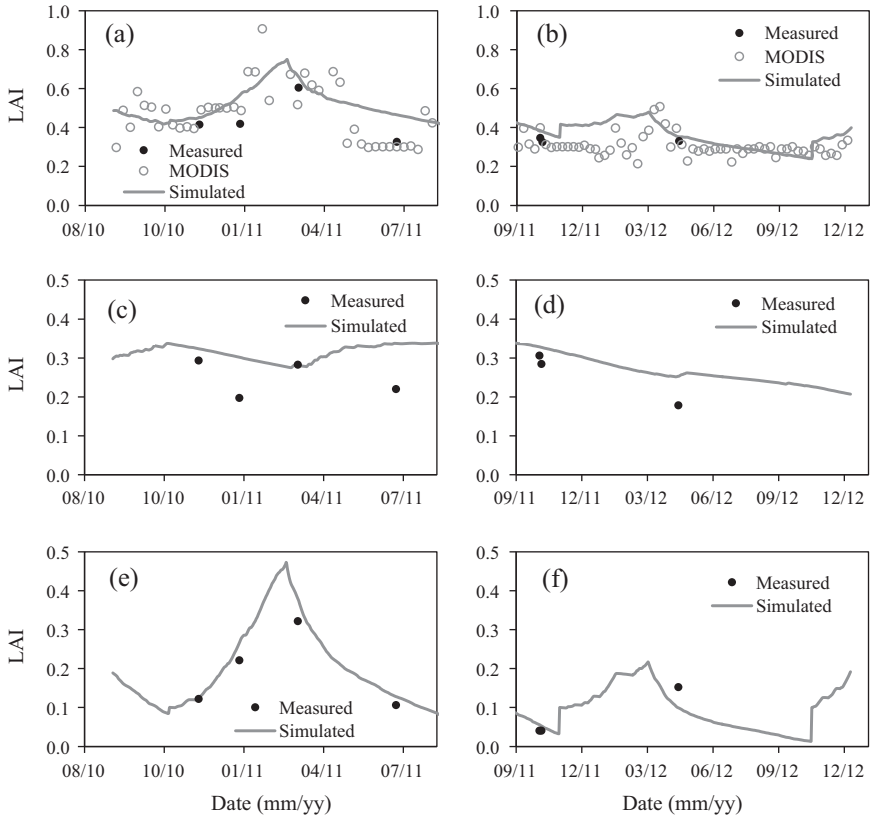

Fig. 2. Comparison of total leaf area index (LAI) from digital photography (measured), MODIS and that of simulations from 3 September 2010 to 31 August 2011 (a) and from 1 September 2011 to 31 December 2012 (b). Comparison of measured and simulated component contributions of canopy LAI from 3 September 2010 to 31 August 2011 (c) and from 1 September 2011 to 31 December 2012 (d) and understory LAI from 3 September 2010 to 31 August 2011 (e) and from 1 September 2011 to 31 December 2012 (f).

2.3. Forcing energy-balance closure

Studies of the surface energy balance showed that surface energy fluxes ($\lambda E + H$; λE: latent heat; H: sensible heat) were frequently underestimated by about 10–30% relative to the surface available energy (Rn–G–S; Rn: net radiation; G: soil heat flux; S: overstory heat storage) (Constantin et al., 1998; Barr et al., 2000, 2001; Wilson et al., 2002; Li et al., 2005). A close examination of flux data measured in the current study revealed that 24 h average closure rate (D) [$D = (H + \lambda E)/(\mathrm{Rn}-\mathrm{G}-\mathrm{S})$] was 74% without accounting for canopy heat storage, which was expected to be relatively minor in short canopies with minimal biomass (Wilson et al., 2002). Wilson et al. (2002) accepted flux data for analysis when canopy heat storage was missing, provided that the vegetation height was less than 8 m, as observed at our Mulga site. The use of flux data to validate biophysically-based models requires that conservation of energy is satisfied (Twine et al., 2000). Therefore, the measured energy budget must be closed by some method. Here the energy balance was closed each half-hourly period by using the Bowen ratio closure method as described by Sugimoto et al. (1997) and Twine et al. (2000), through which the residual energy ($\mathrm{Rn}-\mathrm{G}-H-\lambda E$) was attributed to both H and λE according to the observed Bowen ratio ($H/\lambda E$) for that half hourly period.

2.4. WAVES model

WAVES (Water Atmosphere Vegetation Energy and Solutes) is a coupled water and carbon ecohydrological model that predicts dynamic interactions within the soil–vegetation–atmosphere system at a daily time step (Dawes and Hatton, 1993; Zhang et al., 1999b). The model is able to simulate soil water movement in both the unsaturated and saturated zones using a fully finite difference numerical solution of the Richards equation (Berry et al., 2005). Modelling of the unsaturated zone using the Richards equation allows water movement in the soil profile to be modelled under dry conditions. For each soil type, an analytical soil model proposed by Broadbridge and White (1988) was employed to describe the relationships among water potential, volumetric water content and hydraulic conductivity. Evapotranspiration was estimated by the Penman–Monteith approach (Monteith and Unsworth, 2008). Leaf stomatal conductance was calculated by the equation developed by Ball and Leuning (Ball, 1987; Leuning, 1995), which was scaled to canopy scales using the method proposed by Sellers et al. (1992). The micrometeorological feedback of the sensitivity of transpiration to a marginal change in stomatal conductance at the stand level is regulated by a dimensionless decoupling coefficient proposed by McNaughton and Jarvis (1991). The rate of plant growth in the presence of different availabilities of light, water and nutrients was estimated by an integrated rated methodology of Wu (1994), which is an empirical model without resolving the details of chemical and mechanical controls on photosynthesis. Water is extracted for transpiration by roots, which are distributed along the root profile according to root density distribution and water availability in each soil node (Ritchie et al., 1986). The WAVES model is able to simulate plant physiology, which allows changes in environmental factors (temperature, solar radiation, rainfall) to impact water use by vegetation and recharge. WAVES predicts the dynamic interactions and feedbacks between these processes. Thus, the model is well suited to investigations of hydrological and ecological responses to changes in land management and climatic variation. WAVES emphasises the physical aspects of soil water fluxes physiological control of water loss

through transpiration. It can be used to simulate the hydrological and ecological effects of scenario vegetation management options (e.g. for recharge control), or the water balance implications of changed climatic conditions. A more detailed modelling strategy and description of WAVES is provided in Dawes et al. (1998), Zhang and Dawes (1998) and Zhang et al. (1999b). Most recently, WAVES has successfully reproduced field observations at a point scale (Dawes et al., 2002; Crosbie et al., 2008; Martin et al., 2008; Cheng et al., 2014) and has been used to investigate trends in recharge under different soil and vegetation combinations at regional scales (Barron et al., 2012).

WAVES requires three types of data for parameterisation: meteorology, soil and vegetation. The meteorological data required include daily maximum and minimum temperatures, average vapour pressure deficit, precipitation, precipitation duration, and total solar radiation. The soil data include information on soil layering, along with several hydraulic parameters: soil water conductivity K_s (m d^{-1}), saturated water content θ_s (cm^{-3} cm^{-3}), air-dry volumetric water content θ_d (cm^{-3} cm^{-3}), length of capillary λ_c (m), and characteristic soil water retention curve C. The Broadbridge–White soil model was used to generate a file containing a table of values of soil–water potential, water content, and hydraulic conductivity to allow WAVES to simulate the movement of soil water with the Darcy–Richard's equation.

2.5. Model evaluation and application

2.5.1. Model calibration and validation

There are 26 vegetation parameters in the WAVES model, which control growth, carbon allocation and physiological and phenological responses of vegetation to different environmental conditions (Table 2). Before model calibration, prior vegetation parameters for the Mulga site were adapted from the recommended values for eucalypt trees and for summer annual pastures for the understory habitats contained in the WAVES manual (Dawes et al., 1998). Then, following calibration against MODIS and observed LAI, field-measured soil water content and ET during September 2010–August 2011, some of these parameters for vegetation attributes and water balance components, including the weighting factors for water and nutrient, optimum temperature, light extinction coefficient, maximum carbon assimilation rate, above-ground partition factor, leaf respiration coefficient, specific leaf area, degree-daylight hours were calibrated. Other parameters such as canopy albedo, saturation light intensity, maximum plant available soil moisture, stem and root respiration were estimated from available data or adopted from the literature (Dawes et al., 1998). The subsequently derived values for the Mulga and understory are listed in Table 2. The calibrated model was then validated using the experimental eddy covariance flux data during September 2011–December 2012.

2.5.2. Model performance evaluation

The performance of the WAVES model was evaluated by comparing simulated LAI, soil water content and ET with the corresponding measurements, using three statistical parameters. These were: (1) the coefficient of determination for $y = \alpha x + \beta$ line (r^2); (2) root mean square error (RMSE), providing a measure of the relative average difference between the model estimates and measurements; (3) mean relative error (MRE), providing the bias of the simulated versus observed values; and (4) model efficiency (ME, Nash and Sutcliffe, 1970), presenting variation in measured values accounted for the model:

$$\mathrm{RMSE} = \frac{\sqrt{\frac{1}{n}\sum_{i=1}^{n}(P_i - O_i)^2}}{\overline{O_i}} \quad (1)$$

$$\mathrm{MRE} = \frac{1}{n}\sum_{i=1}^{n}\frac{(P_i - O_i)}{O_i}100\% \quad (2)$$

$$\mathrm{ME} = 1 - \frac{\sum_{i=1}^{n}(P_i - O_i)^2}{\sum_{i=1}^{n}(O_i - O_{avg})^2} \quad (3)$$

Table 2
Derived parameter values for the canopy and understory.

Parameter	Unit	Meaning	Mulga	Understory
1 minus albedo of the canopy	–	A measure of the radiation that can be used by the canopy	0.75	0.75
1 minus albedo of the soil	–	A measure of the radiation that drives soil evaporation	0.80	0.80
Rainfall interception coefficient	–	Rain can be intercepted by a unit of canopy	0.0001	0.0001
Light extinction coefficient	–	Describing bulk exponential decay of light through the plant canopy	−0.65	−0.50
Maximum carbon simulation rate	kg C^{-2} d^{-1}	Maximum amount of carbon that can be assimilated	0.02	0.01
Slope parameter for the conductance model	–	Regulating the amount of production to canopy conductance.	1.0	0.8
Maximum plant available soil water potential	m	Driest water potential for plant roots extracting water from soil	−150	−150
IRM (Integrated rate methodology) weighting of water	–	The weighting factor applied to the availability of water relative to light	2	2
IRM weighting of nutrients	–	The weighting factor applied to the availability of nutrients relative to light	0.2	0.2
Ratio of stomatal to mesophyll conductance	–	Scaling the conductance to CO_2 to that to water vapour	0.02	0.8
Temperature when the growth is 1/2 of optimum	°C	Air temperature when plant growth rate is half of optimum	15	25
Temperature when the growth is optimum	°C	Air temperature when plant growth rate is optimum	17	30
Year day of germination	d	Year day for an annual plant to emerge	−1	310
Degree-daylight hours for growth	°C h	The length of the growing season of an annual plant	−1	47000
Saturation light intensity	μ mol m^{-2} d^{-1}	Light intensity when plant growth rate is optimum	1200	1800
Maximum rooting depth	m	Maximum depth the plant can grow roots	4	0.75
Specific leaf area	LAI kg C^{-1}	The ratio of the leaf area index to the mass of carbon in the canopy	17.5	24
Leaf respiration coefficient	kg C kg C^{-1}	The assimilated carbohydrates used to keep alive the mass of leave	0.0004	0.0004
Stem respiration coefficient	–	The assimilated carbohydrates used to keep alive the mass of stem	0.0001	−1
Root respiration coefficient	–	The assimilated carbohydrates used to keep alive the mass of root	0.0001	0.0001
Leaf mortality rate	Fraction of C d^{-1}	The proportion of leaf carbon lost	0.0004	0.0002
Above-ground partitioning factor	–	The maximum proportion of carbon allocated to above-ground resources	0.15	0.3
Salt sensitivity factor	–	The sensitivity of plant roots to dissolved salt	0.5	0.5
Aerodynamic resistance	s m^{-1}	Determining actual transpiration	20	20

where O_i is the ith observed value, P_i is the ith simulated value, O_{avg} is the average value of the observations and n is the total number of data pairs.

2.5.3. Model application

After validation, the WAVES model was run with historical climate data (1981–2012) to assess effects of climate variability on vegetation growth, water use and the corresponding controls on drainage below 4 m of the soil profile, which is assumed to be the limit to Mulga and pasture root depth. The drainage below the bottom of 4 m soil column is hereafter assumed to become groundwater recharge. During years when ET represented less than 100% of annual precipitation, the remainder of the water budget deficit drained below the bottom of the model (4 m) because runoff is only local in Mulga woodlands on very flat terrain, such as at this site (0.2%; Cleverly et al., 2013; Eamus et al., 2013). The parameter values of vegetation (Mulga and understory), soil and initial conditions for model calibration were used. The simulations were undertaken for both the Mulga and understory. The 32 years of historical climate data for Territory Grape Farm (http://www.bom.gov.au) were obtained from SILO (Jeffrey et al., 2001), an enhanced climate database hosted by the Queensland Climate Change Centre of Excellence.

3. Results and discussion

3.1. Model calibration and validation

In general, simulations of total LAI followed the seasonal patterns of both observed total LAI and MODIS LAI well (Fig. 2a and b). MODIS derived landscape LAI generally ranged between 0.22 and 0.90 during the study period, with a single peak value between late February and early March for each year (0.90 in 2011 and 0.51 in 2012). Simulated total LAI ranged between 0.24 and 0.75 and reached a single peak between late February and early March (0.75 in 2011 and 0.48 in 2012), which was comparable to MODIS trends and ranges. The model was able to explain about 54% of the variation in MODIS LAI (0.10 RMSE) (Table 3).

Good agreement was also obtained between simulated LAI of the overstory and understory and the corresponding LAI field observations (Fig. 2c–f). The model explained about 93% of the variation in observed understory LAI (0.04 RMSE). An abrupt decrease in observed overstory LAI occurred in late January 2011 (Fig. 2c), even with the receipt of substantial precipitation (Fig. 3), possibly because of measurement error in the photos or too few replicates in the number of images captured to provide an accurate assessment of the spatially highly variable LAI. When this single value was excluded, the overall performance of the model in simulating overstory LAI explained 65% of its variation (0.05 RMSE, Table 3). In this simulation, LAI was calibrated to maintain a match between modelled and measured values of ET, resulting in a smaller r^2 with overstory LAI than in the understorey (Table 3) due to extreme variability in leaf physiology, water status and responses to moisture and heat stress of Mulga as a "stress endurer" (Winkworth, 1973; O'Grady et al., 2009; Cleverly et al., 2013; Eamus et al., 2013).

Table 3
The coefficient of determination, root mean square error (RMSE), mean relative error (MRE) and model efficiency (ME) of simulated LAI, soil water and ET.

Item	r^2	RMSE	MRE (100%)	ME
Total LAI (MODIS)	0.54	0.10	18	0.41
Understory LAI (observed)	0.93	0.04	13.3	0.85
Canopy LAI (observed)	0.65	0.05	18.6	0.77
Soil water	0.70	0.03 cm^{-3} cm^{-3}	13.8	0.65
ET	0.90	1.07 mm d^{-1}	10.4	0.93

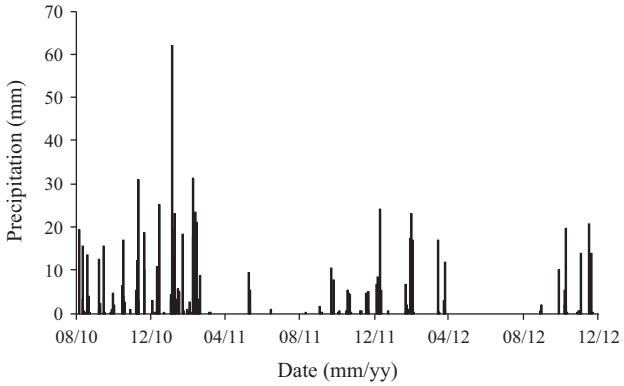

Fig. 3. Daily precipitation measured at the study site during September 2010–December 2012.

Without considering natural variability in physiological parameters, the overall performance of the model was very satisfactory.

In general, soil water content (10- and 60-cm depths) and ET were simulated very well, although there were notable periods when the model did not match the measurements (Figs. 4 and 5). The preceding increase in simulated soil water compared to the observed one in the surface was possibly because the model is unable to capture the effects of biological crusts formed in the *Acacia* savanna woodland (Eamus et al., 2013), which slows down precipitation infiltration into the soil. The model was able to explain about 70% of the variation in soil water content (0.03 m^{-3} m^{-3} RMSE) during the experimental period (Table 3). Likewise, the model explained about 96% of the variation in cumulative ET with an RMSE of 1.07 mm d^{-1} (Table 3). Most importantly, ET and soil moisture content were largest in the summer, smallest in the winter, and followed a pulse-response pattern regardless of season (cf. Figs. 3–5). These results are consistent with a previous study at this site, wherein ET responded with a large, rapid increase after rainfall pulses larger than 2.5 mm, which was followed immediately by exponentially declining ET (Eamus et al., 2013). However, the model used in this study tended to overestimate the magnitude of soil water content responses to rainfall, particularly when precipitation was very high (October 2010–January 2011, Figs. 3 and 4). In contrast, daily values of measured ET (0–5.9 mm) were marginally larger than simulated values (0–5.1 mm). Notwithstanding differences between simulated values and measurements, the model matched measurements of ET and soil water content very well.

We conclude from these results that the calibrated WAVES model is effective at simulating the responses of vegetation water-use and recharge in the study area, particularly with the climate variability in the region. Thus, WAVES was found to provide a reliable framework for evaluating ecohydrological responses of soil and vegetation to large-scale variations in climate.

3.2. Climate variations from 1981 to 2012

Climate in the last 30 years (1981–2012) varied with large fluctuations in precipitation (97–833 mm yr^{-1}; Fig. 6). Variations in mean annual mean temperature (21.2–23.4 °C), solar radiation (20.7–23.1 MJ m^{-2} d^{-1}) and VPD (1.3–2.1 kPa) were uniformly low during years when precipitation was large (Fig. 6). The large variation in annual precipitation supply is typical of central Australia, where two types of storm systems generate moisture: the Australian low and the monsoon depression. The probability of receiving precipitation from either storm system is small (Berry et al., 2011), which was shown in the years when annual rainfall

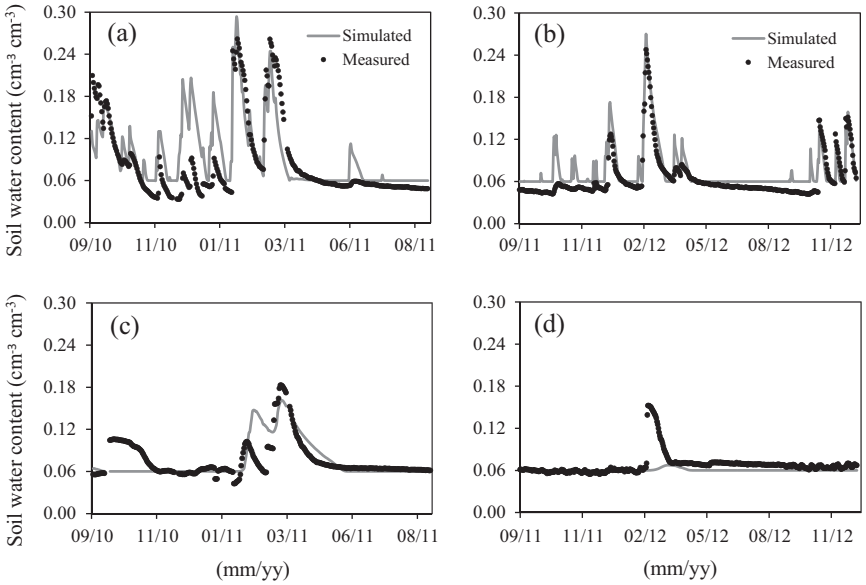

Fig. 4. Comparison of measured and simulated soil water content at 10 cm (a) and 60 cm (c) depths from 3 September 2010 to 31 August 2011 and at 10 cm (b) and 60 cm (d) depths from 1 September 2011 to 31 December 2012.

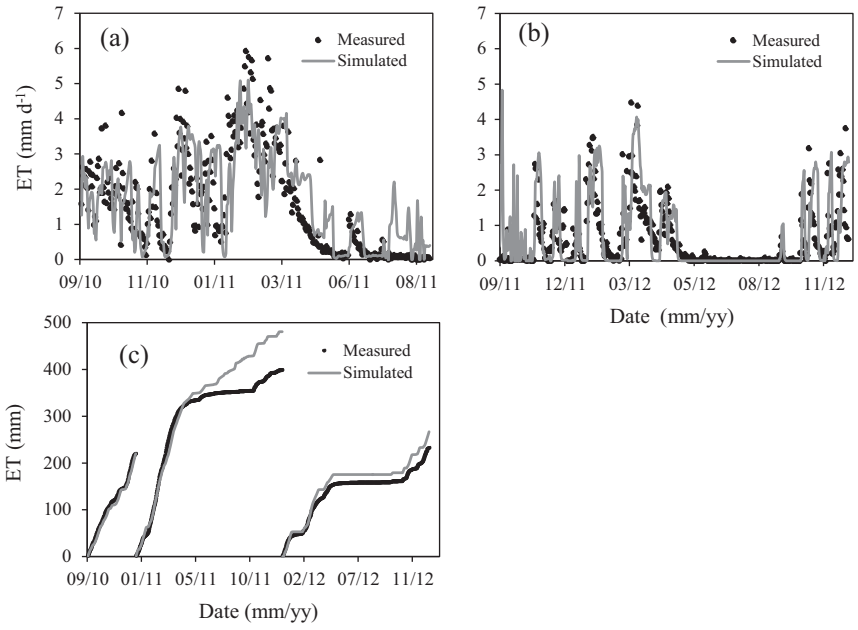

Fig. 5. Comparison of measured and simulated daily ET from 3 September 2010 to 31 August 2011 (a) and from 1 September 2011 to 31 December 2012 (b) and cumulative ET from 3 September 2010 to 31 December 2012 (c).

was less than 100 mm (Fig. 6). However, when both types of storm systems occur simultaneously, extraordinarily large amounts of precipitation can be received (Kong and Zhao, 2010), thereby causing the eightfold range in rainfall shown in Fig. 6. The negative temporal correlation of precipitation against radiation, temperature and VPD indicates the ameliorating effects of cloudiness, rainfall and evaporative cooling on summer temperature regimes (Cleverly et al., 2013). Interestingly, a decreasing trend in precipitation was seen since 2000 although the precipitation in 2010 was extremely high.

Fig. 7 shows the large monthly variability in climatic conditions. Monthly mean temperature and solar radiation were highly seasonal: temperature ranged between 13.6 and 29.8 °C in July and January, respectively (Fig. 7a), while solar radiation ranged from 15.9 to 26.2 MJ m^{-2} over the same period (July–January; Fig. 7b). Precipitation was also highly seasonal, with more than 50% of precipitation falling in the three summer months (wet season, December–February) and more than 80% falling during the monsoon season (November through April; Fig. 7c). Interestingly, VPD in the wet season was almost three times larger than in the dry season (June–August; Fig. 7d) due to high temperatures that compensated for the large absolute humidity during the summer. In contrast, VPD in the tropical savannas of northern Australia are smaller in the wet season than during the dry season, even though the range of mean monthly VPD values are similar in both locations (Fig. 7; Whitley et al., 2011). The continental climate at this site is characterised by a distinct summer wet season, a large difference between winter and summer temperatures, and the large values

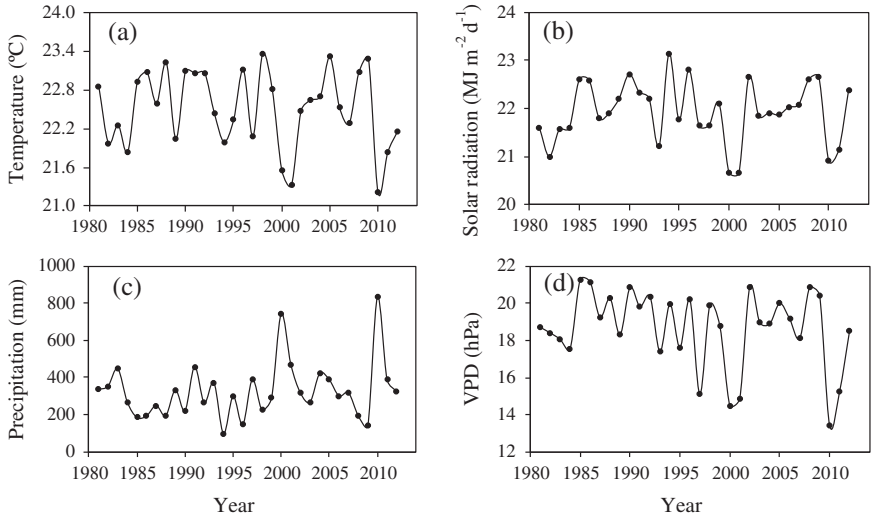

Fig. 6. Annual mean temperature (a), annual mean solar radiation (b), annual precipitation (c) and annual mean vapour pressure deficit (VPD, d) during 1981–2012.

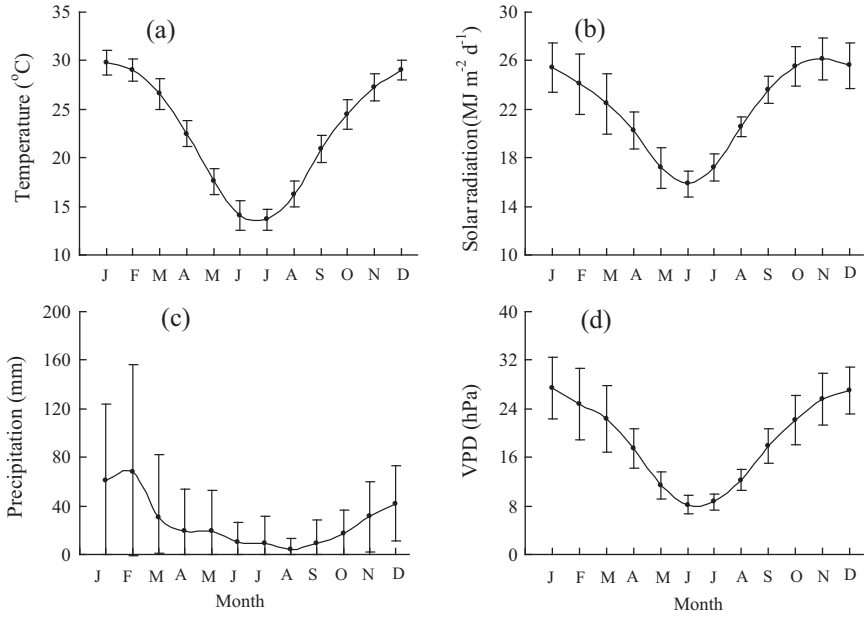

Fig. 7. Mean monthly air temperature (a), mean monthly solar radiation (b), monthly precipitation (c) and mean monthly vapour pressure deficit (VPD, d).

of insolation that occur in tropical semi-arid regions (Fig. 7), where the occurrence of cloud-free conditions is common even during the wet season (Cleverly et al., 2013).

3.3. Vegetation growth affected by climate variability

Fig. 8 illustrates inter-annual variations in simulated annual mean LAI of the overstory and understory during 1981–2012. Due to large inter-annual climate variability (Fig. 6), simulated LAI of both the canopy and understory also displayed large inter-annual variations. Simulated LAI of the overstory ranged from 0.12 to 0.35 with an average of 0.25, while that of the understory ranged from 0.07 to 0.21 with an average of 0.13. Interestingly, an obvious decreasing trend was shown in simulated understory LAI (Fig. 8), reflecting the effect of the extended recent drought (Fig. 6). Due to strong seasonal variation in climate, especially precipitation and temperature (Fig. 7), seasonal variation in simulated understory LAI was large, ranging from 0.03 in September to a maximum of 0.36 in February (Fig. 9c). In contrast, simulated tree canopy LAI showed only a small range in seasonal variation, ranging from 0.22 to 0.28 (Fig. 9a), reflecting the evergreen drought- and heat-tolerant sclerophyllous nature of *Acacia* phyllodes (Eamus et al., 2013). The "bulge" in the simulated understory LAI from November through March (Fig. 9c) coincided with the wet season (Fig. 7c) and reflects the precipitation dependent understory of forbs, shrubs and grasses, the latter of which are comprised of species using the C_3 and C_4 photosynthetic pathways. These responses of the understory to rainfall predominantly determine the intra-annual variation in total LAI (Fig. 9c), as has been noted recently in a field study of this site (Eamus et al., 2013).

The different responses of the tree canopy and understory LAI to climate variations illustrates that the growth of Mulga and understory is responsive to different driving factors. At the inter- and intra-annual scales, variations in simulated LAI of the *Acacia* were equally uncorrelated to temperature, solar radiation, precipitation and VPD, with no single factor showing a significant correlation

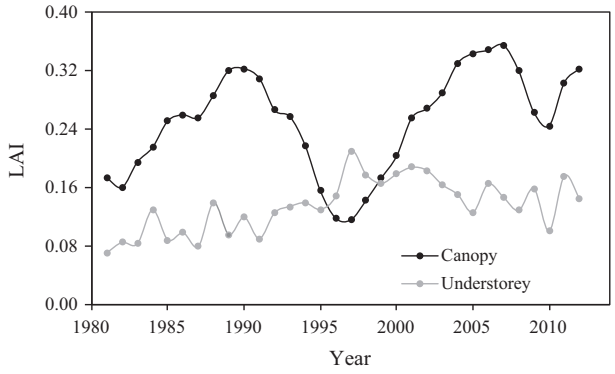

Fig. 8. Simulated annual mean LAI of the canopy and understory from 1981 to 2012.

coefficient (Table 4). In contrast, understory LAI responded positively to smaller VPD and lower temperature at the intra-annual time scale (Table 4). These negative correlations at the inter-annual time scale are indicative of the negative correlation between temperature and precipitation at this site (Section 3.2). In contrast, intra-annual variation in understory LAI were positively and significantly correlated to temperature and precipitation (Table 4), For the understory, monsoon-season precipitation was the most important factor driving variation in LAI, in agreement with extensive analyses by Ma et al. (2013), who compared phenological patterns along the 1100 km North Australian Tropical Transect.

3.4. Vegetation and climate interactions: vegetation water-use controls recharge

Simulated vegetation water-use displayed strong seasonal variations (Fig. 9b and d), as recently observed in eddy covariance data for this site (Eamus et al., 2013). In Mulga, the largest rate of water-use occurred during early summer (December and January), reflecting the influence of summer rainfall, high temperature and large VPD in these months (Fig. 7). In the understory, the largest rates of water use occurred in late summer (February) reflecting summer rainfall, high temperatures, large VPD and the increases in understory LAI that occurred throughout the summer (Fig. 9c). These simulations demonstrate (a) that the major drivers of

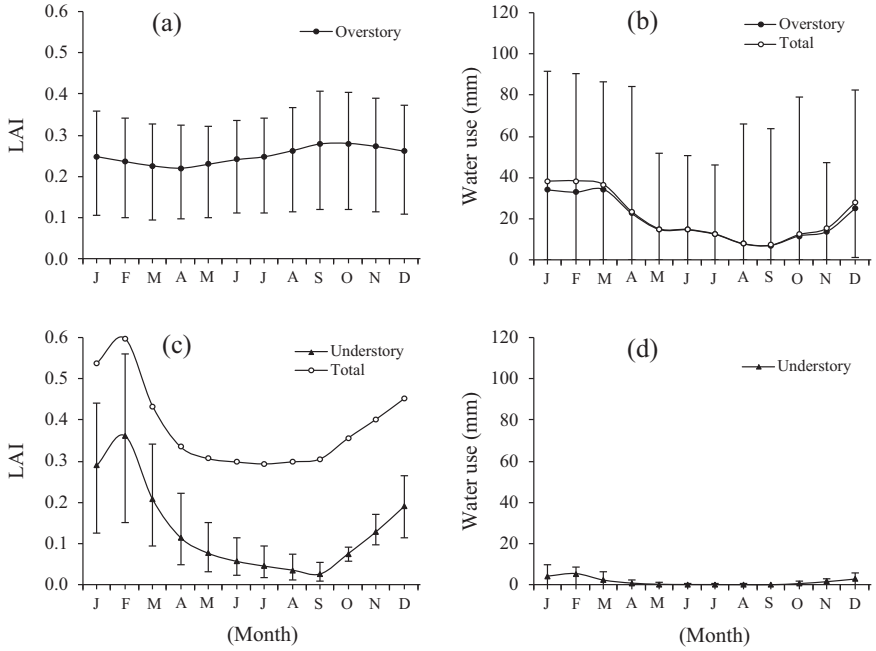

Fig. 9. Simulated monthly mean LAI of the overstory (a), understory and their total (c); simulated monthly water use of the Mulga and the total of Mulga and understory (b) and understory (d).

Table 4
Pearson correlation coefficients between climate variables and vegetation (LAI) or recharge.

Time scale	Climate variables	LAI		Recharge with vegetation
		Canopy	Understory	
Inter-annual	Mean temperature	0.11	−0.15	−0.33
	Solar radiation	0.17	0.17	−0.34
	Rainfall			
	Total amount	0.01	0.03	0.26
	Intensity	–	–	0.06
	VPD	0.08	−0.28	−0.22
Seasonal	Mean temperature	0.08	0.80**	–
	Solar radiation	0.52	0.50	–
	Precipitation (total amount)	−0.20	0.97**	–
	VPD	0.23	0.72**	–

VPD, vapour pressure deficit.
** Correlations are significant with $p < 0.01$.

seasonal changes in vegetation water-use are different for the understory and overstory; and (b) the importance of vegetation dynamics in controlling the partitioning of water fluxes between ET and recharge in this arid region.

Reliable estimates of vegetation water-use and recharge are critical for evaluation and optimal management of water resources. The importance of climate and vegetation in controlling the components of the water cycle at this Mulga site is shown by the simulations of vegetation water-use and groundwater recharge as a function of climate for the period 1981–2012 (Figs. 9 and 10). Annual water-use showed large year-to-year variability for both Mulga and understory; varying from 54 to 584 mm for the Mulga and from 3 to 35 mm for the understory. Mean annual water-use by the Mulga and understory was 232 and 19 mm, respectively (Fig. 10). Total annual water-use by vegetation ranged from 64 to 601 mm, representing 44–100% of annual precipitation (Fig. 6c and Fig. 10).

Fig. 11 shows the simulated annual recharge, with and without vegetation, at the Mulga site during 1981–2012. Annual recharge varied greatly and ranged from 0 to 48 mm, with an average of 6 mm, representing 1.8% of precipitation on average. Due to large climate variability, the simulated values of recharge without vegetation effects ranged from 58 to 672 mm with an average of 236 mm. This accounted for 18–100% of annual precipitation, highlighting the importance of vegetation for controlling recharge. Moreover, the difference in annual recharge between simulations that did and did not include the presence of vegetation was much smaller in dry years than in wet years (data not shown), which indicates the ability of vegetation to reduce recharge in water-limited environments. These values assume that permeability of the soil is equivalent in vegetated and un-vegetated patches. However, bare soil patches are common in Mulga as surface expressions of an impermeable hardpan from which local redistribution of rainfall creates run-on zones beneath the vegetation (Dunkerley and Brown, 1995; Ludwig et al., 2005).

There was almost no recharge when annual precipitation was less than 400 mm, which is nearly 100 mm above average (306 mm; http://www.bom.gov.au), and very little recharge (less than 6 mm, annual mean average) occurred in almost 70% of years (Fig. 12a). For example, there was about 47.6 mm of recharge in 2001 when annual rainfall was 470.9 mm (circled with open circle; Fig. 12a) but there was no recharge in 1991 when rainfall was 458.7 mm (circled in Fig. 12a). This large difference in recharge despite similar annual rainfall is likely to be because of the effect of carry-over of soil water from one year to the next. In 2000, there was about 743.3 mm of rainfall (Fig. 6c), which exceeded water demand by vegetation and thus excess rainfall was stored in the soil and in the following year rain was received by a wet soil profile and this "pushed" recharge to deeper layers. In contrast, in 1990, there was only 221.0 mm which, was almost entirely used by vegetation (Fig. 10). As a result, rain in 1991 was received by a much drier soil profile and water not used by vegetation was stored in the soil instead of generating recharge. Such a carry-over effect has previously been demonstrated in semi-arid grasslands and woodlands (Flanagan et al., 2011; Raz-Yaseef et al., 2012). Furthermore, possibly due to the rapid response of Mulga to precipitation and the relative small amount of simulated recharge compared to precipitation, rainfall intensity does not show significant effects on recharge (Fig. 12b). However, it is noteworthy that rainfall intensity has been identified an important climate factor controlling recharge (Mileham et al., 2009), which emphasis that, under future climate an increase or decrease in rainfall intensity alone could have a significant impact on recharge dynamics in arid environments, even without a change in total rainfall. The coefficient of

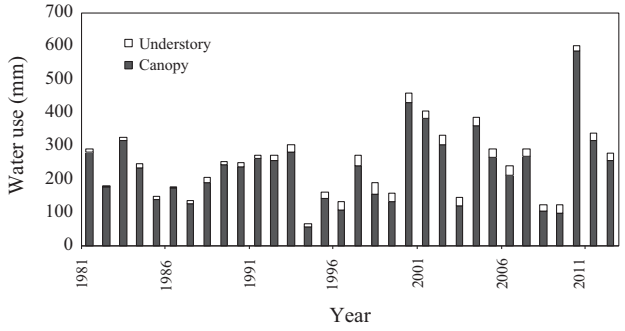

Fig. 10. Simulated annual water use by the Mulga and understory from 1981 to 2012.

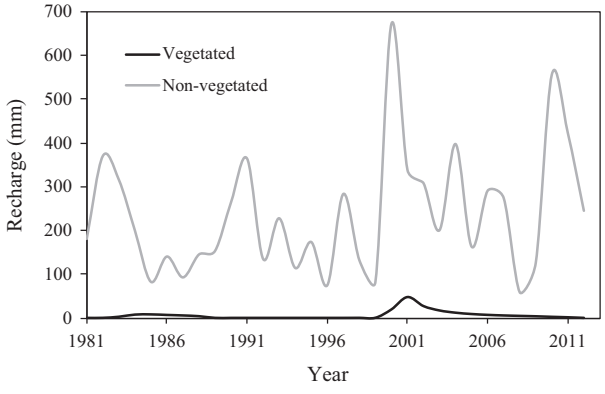

Fig. 11. Simulated annual recharge with vegetation (vegetated) and without vegetation (non-vegetated) during 1981–2012.

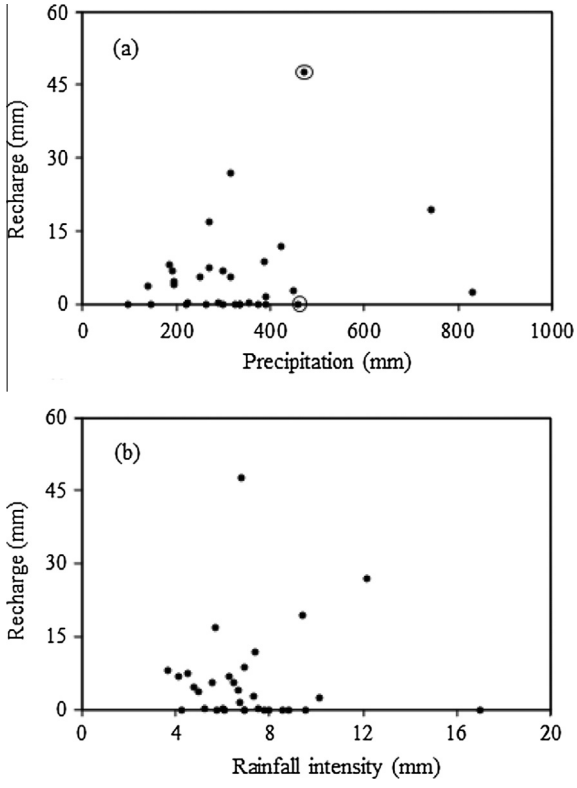

Fig. 12. Relationships between annual recharge and annual precipitation (a) or rainfall intensity (b) during 1981–2012. Rainfall intensity is calculated by computing the moving average of the daily rainfall series applying a 7-day window, and then aggregating the averaged rainfall values that were above a threshold of 5 mm d^{-1} (e.g., Barron et al., 2012).

variation (CV) of simulated annual recharge was 1.67, much larger than that of annual precipitation (CV = 0.47). This indicates that annual recharge was more variable than annual precipitation and this is most likely due to water-use by vegetation. The simulated recharge showed little seasonal variations due to low values as a result of precipitation used by vegetation (Fig. 13).

Simulated recharge was not significantly affected by any single climatic variable (temperature, solar radiation, rainfall, rainfall intensity or VPD; Table 4). This occurs because all of these factors in combination determine (a) rates of ET at daily and seasonal scales (Whitley et al., 2009); (b) seasonal patterns in LAI (Ma et al., 2013); and (c) from the interaction of (a) and (b), partitioning of rainfall into transpiration, soil evaporation and deep drainage (Figs. 8, 10, 11).

Absolute values of fluxes estimated by our model are subject to some uncertainty, although the temporal patterns which are of primary interest in this paper are likely to be reliable. In particular, previous studies in the Ti-Tree Basin have estimated spatially and temporally averaged recharge of approximately 2 mm yr^{-1}, although much of this might occur as infiltration through ephemeral streams with negligible recharge across other areas of the basin (Harrington et al., 2002). Uncertainties in model predictions arise due to errors in model parameters and due to simplifications inherent in the way that the model represents the hydrological system (often termed structural errors). In this study, drainage below 4 m has been equated with recharge, although the rooting depth of mulga remains somewhat uncertain. If it is deeper than 4 m, then a lower mean recharge flux would be calculated (data not shown). The absolute values of recharge will also be sensitive to soil hydraulic parameters. Although these are able to be partially determined through calibration to observed water content data, water content data are not available below 1.2 m, and this also introduces some uncertainty in the drainage rate. Precipitation has been measured with a tipping-bucket rain gauge, which has some local random errors in precipitation measurements (Ciach, 2003) and arid zone precipitation is also highly spatially variable (Lemos et al., 2002). This will also affect the absolute value of drainage.

Our results demonstrate that climate-vegetation interactions exert strong controls on rates of recharge through their impact on LAI and hence vegetation water-use. Knowledge of the interactions amongst all three factors and their controls on groundwater recharge can be used to assess potential impacts of climate variability and land use/land cover change on vegetation health and groundwater availability and has a regional application to management of groundwater resources. Our analyses did not show obvious relationship between modelled recharge and rainfall amount and rainfall intensity (Fig. 12). Inter-annual variability in rainfall is magnified 2- to 4-times in variability in modelled recharge. This indicates that, for an adequate water resources assessment, there is a need to account for the effects of historical variability in climatic conditions and vegetation dynamics on renewable groundwater resources. As the effect of vegetation on groundwater recharge is significant (Fig. 11), it is likely that if land use was to change significantly in response to climate change, the indirect effect of climate change on recharge may be larger than changes in rainfall or temperature. Thus, understanding vegetation response to inter-annual variability of climate should be central in any attempt to predict hydrologic change (Troch et al., 2009).

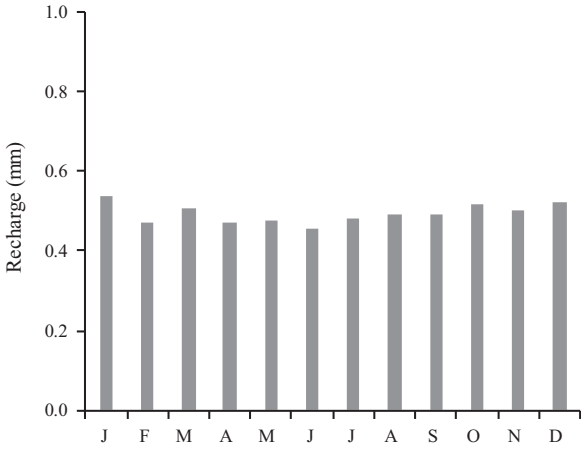

Fig. 13. Simulated monthly recharge with vegetation during 1981–2012.

4. Conclusions

To allocate groundwater resources optimally it is important to consider both the water requirement of vegetation and the interaction of vegetation structure and function and their interactions with climate. Physically-based ecohydrological models are useful tools that can be used to investigate responses of vegetation and the components of a site's water balance to climate variability. In this study, a biophysically based model, WAVES, was applied to examine physiological and hydrological responses of vegetation to climate variations in an arid zone landscape dominated by an *Acacia* (Mulga) savanna woodland. We found that:

(1) The WAVES model was able to reasonably reproduce the dynamics of phenology, vegetation water-use and changes in soil water content in this arid zone landscape. Thus we can use WAVES to investigate the interactions between climate and vegetation and the components of the site's water balance.
(2) Simulated annual mean LAI ranged from 0.12 to 0.35 for the overstory canopy and 0.07–0.21 for the understory, as a result of large inter-annual climatic variability, especially precipitation.
(3) From model simulations with long-term climate data we showed that climate variability greatly affected vegetation water-use and hence groundwater recharge. Simulated annual water-use by vegetation (Mulga & understory) ranged from 64 to 601 mm. The largest rate of vegetation water use was due to high temperature and adequate precipitation in summer months (December to February). Annual recharge when vegetation was excluded from the simulations was highly variable and this variability was mostly dependent on variation in inter-annual precipitation, which ranged from 58 to 672 mm.
(4) Comparison of recharge between with and without vegetation effects indicated that vegetation exerted strong controls on recharge, which was simulated to reduce recharge by between 54 and 653 mm per year. Relative reductions in recharge due to vegetation were larger in dry years than wet years, reflecting the enhanced ability of vegetation to reduce recharge in water-limited environments.
(5) This study provides a deeper insight that improves our understanding of how climate variability and land use/land cover change interactively control recharge. Such an understanding is crucial to improve groundwater management in arid and semi-arid regions.

Acknowledgements

This work was supported by Grants from National Centre for Groundwater Research and Training (NCGRT) and the Australian Government's Terrestrial Ecosystems Research Network (TERN)

(www.tern.gov.au). This work was supported also by OzFlux and the Australian Supersite Network, both parts of TERN and the latter of which is a research infrastructure facility established under the National Collaborative Research Infrastructure Strategy and Education Infrastructure Fund–Super Science Initiative, through the Department of Industry, Innovation, Science, Research and Tertiary Education.

References

Anderson, L., van Klinken, R.D., Shepherd, D., 2008. Aerially surveying Mesquite (*Prosopis* spp.) in the Pilbara. In: A Climate of Change in the Rangelands. Proceedings of the 15th Australian Rangeland Society Biennial Conference, pp. 4. (Australian Rangeland Society: Australia).

Baird, K.J., Stromberg, J.C., Maddock, T., 2005. Linking riparian dynamics and groundwater: an ecohydrologic approach to modeling groundwater and riparian vegetation. Environ. Manage. 36, 551–564.

Ball, J.T., 1987. In: Int. Congress 7th. Prog. Photosynthesis Res. Proc., Providence, 10–15 August 1986, pp. 221–224.

Barr, A.G., van der Kamp, G., Schmidt, R., Black, T.A., 2000. Monitoring the moisture balance of a boreal aspen forest using a deep groundwater piezometer. Agric. For. Met. 102, 13–24.

Barr, A.G., Betts, A.K., Black, T.A., McCaughey, J.H., Smith, C.D., 2001. Intercomparison of BOREAS northern and southern study area surface fluxes in 1994. J. Geophys. Res. 106, 33543–33550.

Barron, O.V., Crosbie, R.S., Dawes, W.R., Charles, S.P., Pickett, T., Donn, M.J., 2012. Climate controls on diffuse groundwater recharge across Australia. Hydrol. Earth Syst. Sci. 16, 4557–4570.

Berg, S.S., Dunkerley, D.L., 2004. Patterned Mulga near Alice Springs, central Australia, and the potential threat of firewood collection on this vegetation community. J. Arid Environ. 59 (2), 313–350.

Berry, S.L., Farquhar, G.D., Roderick, M.L., 2005. Co-evolution of climate, soil and vegetation, encyclopedia of hydrological sciences. In: Anderson, M. (Ed.). John Wiley and Sons, Indianapolis.

Berry, G., Reeder, M.J., Jakob, C., 2011. Physical mechanisms regulating summertime rainfall over northwestern Australia. J. Clim. 24, 3705–3717.

Broadbridge, P., White, I., 1988. Constant rate rainfall infiltration: A versatile nonlinear model: 1. Analytic solution. Water Res. Res. 24, 145–154.

Chen, C., Wang, E.L., Yu, Q., 2010. Modelling the effects of climate variability and water management on crop water productivity and water balance in the North China Plain. Agric. Water Manage. 97, 1175–1184.

Cheng, L., Zhang, L., Wang, Y.P., Yu, Q., Eamus, D., 2014. Quantifying the effects of elevated CO_2 on water budgets by combining FACE data with an ecohydrological model. Ecohydrol. http://dx.doi.org/10.1002/eco.1478.

Ciach, G.J., 2003. Local random errors in tipping-bucket rain gauge measurements. J. Atmos. Oceanic Technol. 20, 752–759.

Cleverly, J., 2011. Alice Springs Mulga OzFlux site. OzFlux: Australian and New Zealand Flux Research and Monitoring Network, hdl: 102.100.100/8697.

Cleverly, J., Boulain, N., Villalobos-Vega, R., Gant, N., Faux, R., Wood, C., Peter, C.G., Yu, Q., Leigh, A., Eamus, D., 2013. Dynamics of component carbon fluxes in a semi-arid *Acacia* woodland, central Australia. J. Geophys. Res.. http://dx.doi.org/10.1002/jgrg.20101.

Clifton, C., Evans, R., 2001. Environmental Water Requirements of Groundwater Dependent Ecosystems, Environmental flows Initiative Technical Report, Report, 2.

Constantin, J., Inclan, M.G., Raschendorf, M., 1998. The energy budget of a space forest: field measurements and comparison with the forest-land-atmosphere model (FLAME). J. Hydrol. 2 (12-213:2), 2–35.

Crosbie, R.S., McCallum, J., Walker, G.R., Chiew, F.H.S., 2008. Diffuse groundwater recharge modelling across the Murray–Darling Basin. A report to the Australian government from the CSIRO Murray–Darling Basin Sustainable Yields project, Water for a Healthy Country Flagship, CSIRO, Canberra, <http://www.csiro.au/files/files/pn7z.pdf>.

Crosbie, R., McCallum, J., Walker, G.R., 2011. The Impact of Climate Change on Dryland Diffuse Groundwater Recharge in the Murray–Darling Basin. National Water Commission.

Dawes, W., Hatton, T.J., 1993. Topog_IRM 1. Model description. CSIRO division of water resources. Tech. Memorandum 93, 33.

Dawes, W.R., Zhang, L., Dyce, P., 1998. WAVES V3.5 User Manual, CSIRO Land and Water, Canberra, ACT.

Dawes, W.R., Gilfedder, M., Stauffacher, M., Coram, J., Hajkowicz, S., Walker, G.R., Young, M., 2002. Assessing the viability of recharge reduction for dryland salinity control: Wanilla, Eyre Peninsula. Aust. J. Soil Res. 40, 1407–1424.

Donohue, R.J., Roderick, M.L., McVicar, T.R., 2007. On the importance of including vegetation dynamics in Budyko's hydrological model. Hydrol. Earth Syst. Sci. Discuss. 11, 983–995.

Dunkerley, D.L., 2002. Infiltration rates and soil moisture in a groved mulga community near Alice Springs, arid central Australia: evidence for complex internal rainwater redistribution in a runoff–runon landscape. J. Arid Environ. 51 (2), 199–219.

Dunkerley, D.L., Brown, K.J., 1995. Runoff and runon areas in a patterned chenopod shrubland, arid western New South Wales, Australia – characteristics and origin. J. Arid Environ. 30, 41–55.

Eamus, D., Hatton, T., Cook, P., Colvin, C., 2006. Ecohydrology: Vegetation Function, Water and Resource Management. CSIRO Publishing, Collingwood.

Eamus, D., Cleverly, J., Boulain, N., Grant, N., Faux, R., Villalobos-Vega, R., 2013. Carbon and water fluxes in an arid-zone *Acacia* savanna woodland: An analyses of seasonal patterns and responses to rainfall events. Agric. For. Met. http://dx.doi.org/10.1016/j.agrformet.2013.04.020.

Farrington, P., Greenwood, E.A.N., Bartle, G.A., Beresford, J.D., Watson, G.D., 1989. Evaporation from Banksia woodland on a groundwater mound. J. Hydrol. 105, 173–186.

Fernandez, J.E., Slawinski, C., Moreno, F., Walczak, R.T., Vanclooster, M., 2002. Simulating the fate of water in a soil–crop system of a semi-arid Mediterranean area with the WAVE 2.1 and the EURO-ACCESS-II models. Agric. Water Manage. 56, 113–129.

Flanagan, L.B., Adkinson, A.C., 2011. Interacting controls on productivity in a northern Great Plains grassland and implications for response to ENSO events. Global Change Biol. 17, 3293–3311.

Garcia, C.A., Andraski, B.J., Stonestrom, D.A., Cooper, C.A., Simunek, J., Wheatcraft, S.W., 2011. Interacting vegetative and thermal contributions to water movement in desert soil. Vadose Zone J. 10 (2), 552–564.

Gee, G.W., Wierenga, P.J., Andraski, B.J., Young, M.H., Fayer, M.J., Rockhold, M.L., 1994. Variations in water balance and recharge potential at three western desert sites. Soil Sci. Soc. Am. J. 58 (1), 63–72.

Gerten, D., Schaphoff, S., Haberlandt, U., Lucht, W., Sitch, S., 2004. Terrestrial vegetation and water balance—hydrological evaluation of a dynamic global vegetation model. J. Hydrol. 286 (1), 249–270.

Guswa, A.J., Celia, M.A., Rodriguez-Iturbe, I., 2002. Models of soil moisture dynamics in ecohydrology: a comparative study. Water Res. Res. 38, 5-1–5-15.

Harrington, G., Cook, P.G., Herczeg, A.L., 2002. Spatial and temporal variability of ground water recharge in central Australia: a tracer approach. Groundwater 40, 518–528.

Hill, S.M., Hill, L.J., 2003. Some important plant characteristics and assay overviews for biogeochemical surveys in western New South Wales. Advances in Regolith. CRC LEME, 187–192.

Jeffrey, S.J., Carter, J.O., Moodie, K.B., Beswick, A.R., 2001. Using spatial interpolation to construct a comprehensive archive of Australian climate data. Environ. Modell. Soft. 16, 309–330.

Jha, M., Chowdhury, A., Chowdary, V., Peiffer, S., 2007. Groundwater management and development by integrated remote sensing and geographic information systems: prospects and constraints. Water Res. Manage. 21, 427–467.

Johnston, R.M., Barry, S.J., Bleys, E., Bui, E.N., Moran, C.J., Simon, D.A.P., Carlile, P., McKenzie, N.J., Henderson, B., Chapman, G., Imhoff, M., Maschmedt, D., Howe, D., Grose, C., Schokneckt, N., Powell, B., Grundy, M., 2003. ASRIS: the database. Aust. J. Soil Res. 41, 1021–1036.

Kong, Q., Zhao, S., 2010. Heavy rainfall caused by interactions between monsoon depression and middle-latitude systems in Australia: a case study. Meteorol. Atmos. Phys. 106, 205–226.

Kucharik, C.J., Foley, J.A., Delire, C., Fisher, V.A., Coe, M.T., Lenters, J.D., Young-Molling, C., Ramankutty, N., 2000. Testing the performance of a dynamic global ecosystem model: water balance, carbon balance, and vegetation structure. Global Biogeochem. Cycles 14, 795–825.

Laio, F., Porporato, A., Ridolfi, L., Rodriguez-Iturebe, I., 2001. Plants in water-controlled ecosystems: Active role in hydrologic processes and response to water stress: II. Probabilistic soil moisture dynamics. Adv. Water Res. 24, 707–723.

Lemos, M.C., Finan, T.J., Fox, R.W., Nelson, D.R., Tucker, J., 2002. The use of seasonal climate forecasting in policymaking: lessons from Northeast Brazil. Clim. Change 55, 479–507.

Leuning, R., 1995. A critical appraisal of a combined stomatal–photosynthesis model for C_3 plants. Plant, Cell Environ. 18, 339–355.

Li, Z.Q., Yu, G.R., Wen, X.F., Zhang, L.M., Re, C.Y., Fu, Y.L., 2005. Energy balance closure at ChinaFLUX sites. Sci. China Ser. D-Earth Sci. 48, 51–62.

Ludwig, J.A., Wilcox, B.P., Breshears, D.D., Tongway, D.J., Imeson, A.C., 2005. Vegetation patches and runoff-erosion as interacting ecohydrological processes in semiarid landscapes. Ecology 86, 288–297.

Ma, X., Huete, A., Yu, Q., Coupe, N.R., Davies, K., Broich, M., Ratana, P., Beringer, J., Hutley, L.B., Cleverly, J., Boulain, N., Eamus, D., 2013. Spatial patterns and temporal dynamics in savanna vegetation phenology across the North Australian tropical transect. Remote Sens. Environ. 139, 97–115.

MacFarlane, C., Hoffman, M., Eamus, D., Kerp, N., Higginson, S., McMurtrie, R., Adams, M., 2007. Estimation of leaf area index in eucalypt forest using digital photography. Agric. For. Met. 143, 176–188.

Martin, M., Silberstein, R., Smettem, K., Xu, C.C., 2008. Identifying Sources of Uncertainty in Groundwater Recharge Estimates Using the Biophysical Model WAVES. In: Lambert, M; Daniell, TM; Leonard, M (Eds). Proceedings of Water Down Under. Modbury, SA: Engineers Australia; Causal Productions, pp. 2161–2169.

McNaughton, K.G., Jarvis, P.G., 1991. Effects of spatial scale on stomatal control of transpiration. Agric. For. Met. 54, 279–302.

Mileham, L., Taylor, R.G., Todd, M., Tindimugaya, C., Thompson, J., 2009. The impact of climate change on groundwater recharge and runoff in a humid, equatorial catchment: sensitivity of projections to rainfall intensity. Hydrol. Sci. J. 54 (4), 727–738.

Monteith, J., Unsworth, M., 2008. Principles of Environmental Physics. Edward Arnold, London, UK, pp. 250.

Morton, S.R., Stafford Smith, D.M., Dickman, C.R., Dunkerley, D.L., Friedel, M.H., McAllister, R.R.J., Reid, J.R.W., Roshier, D.A., Smith, M.A., Walsh, F.J., Wardle,

G.M., Watson, I.W., Westoby, M., 1999b. A fresh framework for the ecology of arid Australia. J. Arid Environ. 75, 313–329.
Nash, J.E., Sutcliffe, J.V., 1970. River flow forecasting through conceptual models part I-A discussion of principles. J. Hydrol. 10, 282–290.
O'Grady, A.P., Cook, P.G., Eamus, D., Duguid, A., Wischusen, J.D.H., Fass, T., Worldege, D., 2009. Convergence of tree water use within an arid-zone woodland. Oecologia 160, 643–655.
Perry, R.A., 1970. The effects on grass and browse production of various treatments on a mulga community in central Australia. In: Proc. 11th int. Grassld Congr., Surfers Paradise, pp. 63–6.
Porporato, A., D'odorico, P., Laio, F., Ridolfl, L., Rodriguez-lturbe, I., 2002. Ecohydrology of water-controlled ecosystems. Adv. Water Res. 25, 1335–1348.
Raz-Yaseef, N., Yakir, D., Schiller, G., Cohen, S., 2012. Dynamics of evapotranspiration partitioning in a semi-arid forest as affected by temporal rainfall patterns. Agric. For. Met. 157, 77–85.
Ritchie, J.T., Kiniry, J.R., Jones, C.A., Dyke, P.T., 1986. Model inputs. In: Jones, C.A., Kiniry, J.R. (Eds.), CERES-Maize: a Simulation Model of Maize Growth and Development. Texas A&M University Press, College Station, pp. 37–48.
Scanlon, B.R., Levitt, D.G., Reedy, R.C., Keese, K.E., Sully, M.J., 2005. Ecological controls on water-cycle response to climate variability in deserts. Proc. Natl. Acad. Sci. U.S.A. 102 (17), 6033–6038.
Sellers, P.J., Berry, J.A., Collatz, G.J., Field, C.B., Hall, F.G., 1992. Canopy reflectance, photosynthesis, and transpiration. III. A reanalysis using improved leaf models and a new canopy integration scheme. Remote Sens. Environ. 42, 187–216.
Singh, S., Kroes, J.G., van Dam, J.C., Feddes, R.A., 2006. Distributed ecohydrological modelling to evaluate the performance of irrigation system in Sirsa district, India: I. Current water management and its productivity. J. Hydrol. 329, 692–713.
Sugimoto, S., Nakamura, F., Ito, A., 1997. Heat budget and statistical analysis of the relationship between stream temperature and riparian forest in the Toikanbetsu River basin, northern Japan. J. For. Res. 2 (2), 103–107.
Thorburn, P.J., Hatton, T.J., Walker, G.R., 1993. Combining measurements of transpiration and stable isotopes of water to determine groundwater discharge from forests. J. Hydrol. 150, 563–587.
Troch, P.A., Martinez, G.F., Pauwels, V.R.N., Durcik, M., Sivapalan, M., Harman, C.J., Brooks, P.D., Gupta, H.V., Huxman, T.E., 2009. Climate and vegetation water use efficiency at catchment scales. Hydrol. Processes 23, 2409–2414.
Twine, T.E., Kustas, W.P., Norman, J.M., Cook, D.R., Houser, P.R., Meyers, T.P., Prueger, J.H., Starks, P.J., Wesely, M.L., 2000. Correcting eddy-covariance flux underestimates over a grassland. Agric. For. Met. 103, 279–300.
Weiss, M., Baret, F., Smith, G.J., Jonckheere, I., Coppin, P., 2004. Review of methods for in situ leaf area index (LAI) determination Part II, Estimation of LAI, errors and sampling. Agric. For. Met. 121, 37–53.
Whitley, R.J., Medlyn, B.E., Zeppel, M.J.B., Macinnis-Ng, C.M.O., Eamus, D., 2009. Comparing the Penman–Monteith equation and a modified Jarvis–Stewart model with an artificial neural network to estimate stand scale transpiration and canopy conductance. J. Hydrol. 373, 256–266.
Whitley, R.J., Macinnis-Ng, C.M.O., Hutley, L.B., Beringer, J., Zeppel, M., Williams, M., Taylor, D., Eamus, D., 2011. Is productivity of mesic savannas light limited or water limited? Results of a simulation study. Glob. Change Biol. 17, 3130–3149.
Wilson, K., Goldstein, A., Falge, E., Aubinet, M., Baldocchi, D., Berbigier, P., Bernhofer, C., Ceulemans, R., Dolman, A.H., Field, C., Grelle, A., Law, B., Meyers, T., Moncrieff, J., Monson, R., Oechel, W., Tenhunen, J., Valentini, R., Verma, S., 2002. Energy balance closure at FLUXNET sites. Agric. For. Met. 113, 223–243.
Winkworth, R.E., 1973. Eco-physiology of Mulga (*Acacia* aneura). Tropical Grasslands 7, 43–48.
Wu, H., Rykiel Jr, E.J., Hatton, T., Walker, J., 1994. An integrated rate methodology (IRM) for multi-factor growth rate modelling. Ecolo. Model. 73, 97–116.
Zhang, L., Dawes W.R. (Eds.), 1998. WAVES–An Integrated Energy and Water Balance Model. Technical Report No. 31/98, CSIRO Land and Water, Canberra, Australia.
Zhang, Y., Schilling, K.E., 2006. Effects of land cover on water table, soil moisture, evapotranspiration, and groundwater recharge: a field observation and analysis. J. Hydrol. 319, 328–338.
Zhang, L., Dawes, W.R., Slavich, P.G., Meyer, W.S., Thorburn, P.J., Smith, D.J., Walker, G.R., 1999a. Growth and ground water uptake responses of lucerne to changes in groundwater levels and salinity: lysimeter, isotope and modelling studies. Agric. Water Manage. 39, 265–282.
Zhang, L., Hume, I.H., O'Connell, M.G., Mitchell, D.C., Mithorepe, P.L., Yee, M., Dawes, W.R., Hatton, T.J., 1999b. Estimating episodic recharge under different crop/pasture rotations in the Mallee region. Part 1. Experiments and model calibration. Agric. Water Manage. 42, 219–235.